Drug Design, Development and Therapy

Dovepress
open access to scientific and medical research

Open Access Full Text Article

ORIGINAL RESEARCH

Paroxetine Attenuates Chondrocyte Pyroptosis and Inhibits Osteoclast Formation by Inhibiting NF-κB Pathway Activation to Delay Osteoarthritis Progression

Xiaohang Zheng[1,2], Jianxin Qiu[1,2], Ning Gao[3], Ting Jiang[1,2], Ze Li[1,2], Weikang Zhang[1,2], Yuhang Gong[1,2], Zhenghua Hong[1,2], Huaxing Hong[1,2]

[1]Orthopedic Department, Taizhou Hospital Affiliated to Wenzhou Medical University, Linhai, People's Republic of China; [2]Enze Medical Research Center, Taizhou Hospital Affiliated to Wenzhou Medical University, Linhai, People's Republic of China; [3]Department of Cardiovascular Surgery, The Second Affiliated Hospital of Zhejiang University School of Medicine, Hangzhou, People's Republic of China

Correspondence: Huaxing Hong; Zhenghua Hong, Taizhou Hospital Affiliated to Wenzhou Medical University, No. 150, Ximen Street, Taizhou City, Zhejiang Province, People's Republic of China, Fax +86 0576-8512-0120, Email tzyyhhx@126.com; 0001hzh@163.com

Background: Osteoarthritis (OA), a common chronic joint disease, is characterized by cartilage degeneration and subchondral bone reconstruction. NF-κB signaling pathway-activated inflammation and NLRP3-induced pyroptosis play essential roles in the development of OA. In this study, we examine whether paroxetine can inhibit pyroptosis and reduce osteoclast formation, thereby delaying the destruction of knee joints.

Methods: We employed high-density cultures, along with quantitative polymerase chain reactions and Western blotting techniques, to investigate the effects of paroxetine on extracellular matrix synthesis and degradation. The expression levels of NF-κB and pyroptosis-related signaling pathway proteins were examined by Western blotting and immunofluorescence. Furthermore, the impact of paroxetine on RANKL-induced osteoclast formation was evaluated through TRAP staining and F-actin ring fluorescence detection. To investigate the role of paroxetine in vivo, we constructed a mouse model with destabilization of the medial meniscus (DMM) surgery. Safranin O-Fast Green staining, Hematoxylin-Eosin staining, and immunohistochemistry were conducted to observe the extent of knee joint cartilage deformation. In addition, TRAP staining was used to observe the formation of osteoclasts in the subchondral bone.

Results: In the in vitro experiments with ATDC5, paroxetine treatment attenuated IL-1β-induced activation of the pyroptosis-related pathway and suppressed extracellular matrix catabolism by inhibiting the NF-kB signaling pathway. In addition, paroxetine treatment decreased the expression of RANKL-induced osteoclast marker genes and reduced osteoclast formation. In animal experiments conducted in vivo, mice treated with paroxetine exhibited thicker knee cartilage with a smoother surface compared to the DMM group. Additionally, the formation of osteoclasts in the subchondral bone was reduced in the paroxetine-treated mice. Further analysis revealed that paroxetine treatment played a role in preserving the balance of the extracellular matrix and delaying knee joint degeneration.

Conclusion: Paroxetine can inhibit pyroptosis and reduce osteoclast formation via inhibiting the NF-κB signaling pathway, suggesting that it may have therapeutic effects in patients with OA.

Keywords: paroxetine, pyroptosis, inflammation, osteoclasts, osteoarthritis

Introduction

Osteoarthritis (OA) is a common degenerative joint disease.[1,2] It manifests as degeneration and damage to joint cartilage, resulting in pain and disability.[3,4] In the current management of OA, conservative treatment often involves the use of analgesics and anti-inflammatory drugs, as well as joint replacement surgery in patients with advanced stages of the disease.[5,6] However, these approaches associate with certain drawbacks; the drug effects are temporary and do not

Received: 5 May 2023
Accepted: 6 August 2023
Published: 16 August 2023

alleviate or stop the progression of OA, while the risks and financial burden need to be considered if surgery is performed.[7] Therefore, it is important to identify new safe, and effective drugs to mitigate or reverse the progression of OA.

The homeostasis of chondrocytes is disrupted in OA, which results in the secretion of proteolytic enzymes, such as ADAM metallopeptidase with thrombospondin type 1 motif 5 (ADAMTS5) and matrix metalloproteinase 3 (MMP3), causing degeneration and damage to articular cartilage.[2,8–10] At the same time, normal subchondral bone provides mechanical assistance and nutritional support to the cartilage, contributing to the stability of the joint structure.[11,12] Osteoclasts are vital in facilitating the structural modifications and remodeling of subchondral bone.[13] Additionally, osteoclasts are actively engaged in the amplification of sensory innervation within the subchondral region and exhibit heightened sensitivity to pain stimuli.[14] The critical role of subchondral osteoclasts in OA progression makes them a suitable target for therapeutic inventions. Recent studies have demonstrated that the nuclear factor kappa B (NF-κB) signaling pathway plays a key role in the initiation and development of chondrogenic and osteolytic changes in OA.[15–17] The inhibition of NF-κB pathway can attenuate chondrocyte apoptosis and delay cartilage degeneration in OA models.[18–20]

Pyroptosis is a pro-inflammatory programmed cell death mechanism.[21] It is characterized by cell swelling and rupture, cell membrane lysis, cytoplasmic content release into the extracellular compartment, and chromosomal DNA breakage.[21,22] The common activation of pyroptosis is mediated by the NOD-like receptor thermal protein domain associated protein 3 (NLRP3) inflammasome, which consists of NLRP3, apoptosis-associated spot-like protein containing CARD (ASC), and pro-caspase 1.[23–25] In this activation pathway, NLRP3 is activated in response to intra- and extracellular stimuli, which results in the recruitment of ASC, the binding of ASC to pro-caspase 1, and the assembly of the NLRP3 inflammasome.[26] Activated NLRP3 inflammasomes cleave pro-caspase 1 to activate caspase 1, which cleaves both interleukin 1 beta (IL-1β) and interleukin 18 (IL-18) precursors and promotes their maturation and secretion.[27]

Paroxetine, a well-known 5-hydroxytryptamine selective reuptake inhibitor, is widely used in the treatment of depression, anxiety disorders, and Alzheimer's disease.[28–30] Recent research has demonstrated that paroxetine can modulate diverse biological mechanisms in inflammatory bowel disease and potentially relieve intestinal inflammation by regulating the composition and functionality of the gut microbiota.[31] In a research conducted on rats with collagen-induced arthritis, the administration of paroxetine proved to be successful in alleviating symptoms, as well as reducing both synovial inflammation and bone destruction.[32] The therapeutic efficacy of G protein-coupled receptor kinase 2 (GRK2) inhibition has been reported to have a significant benefits in patients with OA;[33] however, the underlying molecular mechanism remains unstudied. In this study, we aimed to investigate the chondrocyte-protective and osteoclast-inhibitory effects of paroxetine, and to uncover the molecular mechanism involved.

Materials and Methods

Reagents and Materials

Paroxetine was purchased from Apexbio (Suzhou, China). Alpha-MEM and DMEM were procured from Biosharp (Anhui, China). The IL-1β and Cell Counting Kit-8 (CCK-8) were purchased from Med Chem Express (New Jersey, USA). RANKL and M-CSF were procured from LifeTein (Beijing, China). Primary antibodies against Nlrp3 (ab263899, 1:1000), IL-1β (ab254360, 1:1000), Caspase1 (ab179515, 1:1000) and ADAMTS5 (ab185722, 1:1000) were purchased from Abcam (Cambridge, UK). The aggrecan antibody (PA1-1746, 1:1000) was procured from Thermo Fisher Scientific (Waltham, MA, USA), and MMP3 (ET1705-98, 1:1000) and SOX9 (ET1611-56, 1:1000) antibodies were purchased from Huaan Biotechnology (Hangzhou, China). Primary antibodies against P65 (8242, 1:1000), p-P65 (3033, 1:1000), IκBα (4812, 1:1000), p-IκBα (2859, 1:1000), and β-actin (4970, 1:10,000) were procured from Cell Signaling Technology (Danvers, MA, USA). The NFATc1 antibody (YT5381, 1:1000) was procured from ImmunoWay (Shanghai, China).

Cell Viability and Cytotoxicity Assays

Six-week-old C57 mice were used for the isolation of bone marrow-derived macrophages (BMMs). The bone marrow was washed with Alpha-MEM containing 10% serum and 30 ng/mL M-CSF and cultured in an incubator under conditions of 37°C and 5% CO_2. The medium was changed every other day and the adherent cells were BMMs. The ATDC5 cell line was purchased from the European Collection of Authenticated Cell Cultures and cultured in DMEM containing 5% serum. To investigate the cytotoxic effects of paroxetine, ATDC5 cells were treated with different concentrations of paroxetine for 24 and 48h and the cell counting kit-8 (CCK8) assay was performed according to the manufacturer's instructions. The absorbance at 450 nm of each well was measured with the Multiskan FC microplate photometer (Thermo Fisher Scientific). In another experiment, BMMs were treated with different concentrations of paroxetine for 48 and 96 h and assayed. The 50% inhibition concentration (IC_{50}) of paroxetine were calculated using GraphPad Prism.

Assay of Extracellular Matrix Components

To observe the effects of paroxetine on cartilage production, ATDC5 cells were cultured at high density. After the cells had adhered to the multi-well plates, MEM containing IL-1β and different concentrations of paroxetine was added. The cells were stained with toluidine blue after 7 days of treatment and the multi-well plates were scanned with an Epson V600 Photo Scanner (Japan). In another experiment, ATDC5 cells were treated with IL-1β and different concentrations of paroxetine for 48 h for the extraction of RNA and protein to examine the synthesis and catabolism of extracellular matrix components.

Osteoclast Differentiation and Osteoclast-Related Gene Expression

The effects of paroxetine on osteoclast differentiation in vitro were examined. BMMs were treated with 50 ng/mL RANKL and different concentrations of paroxetine, followed by Tartrate-resistant acid phosphatase (TRAP) staining and filamentous actin (F-actin) ring formation assay. The number and area of osteoclasts were determined for statistical analysis. To observe the time-dependent effects of paroxetine, BMMs at different stages of osteoblast differentiation (1–3 days, 3–5 days, and 5–7 days) were treated with the compound as indicated above.

To investigate the effects of paroxetine on osteoclast marker genes, BMMs were treated with RANKL and different concentrations of paroxetine. After significant osteoclast formation was observed under the microscope, total RNA was extracted for reverse transcription-polymerase chain reaction (RT-PCR). The expression of osteoclast-related genes (c-Fos, NFATC1, ACP5, V-ATPase D2, DC-STAMP, and CTSK) was examined by RT-PCR.

Quantitative Polymerase Chain Reaction

Total RNA was extracted using TRIzol reagent (Gibco, Grand Island, NY, USA), and complementary DNA (cDNA) was synthesized by reverse transcription using the HiFiScript cDNA synthesis kit (CWBiotech, China). Quantitative polymerase chain reactions were performed on an ABI 7300 plus real-time PCR system (Applied Biosystems, Foster City, CA, USA) using the ChamQ Universal SYBR qPCR Master Mix (Vazyme, China) and corresponding primers. GAPDH was used as an internal reference for the normalization of gene expression. The $2^{-\Delta\Delta CT}$ method was used to calculate the relative expression of each gene. Primer sequences for the detection of target genes are shown in Table 1.

Western Blotting

Total proteins were separated with radioimmunoprecipitation assay buffer (Biosharp, Hefei, China) containing 1 mM phenylmethylsulfonyl fluoride and a phosphatase inhibitor cocktail (MedChemExpress, NJ, USA). After centrifugation at 12,000 rpm for 15 min at 4°C, the concentration of proteins was determined with the BCA protein assay kit (AMEKO, Shanghai, China). The proteins (30 μg) were separated by sodium dodecyl sulfate polyacrylamide gel electrophoresis using 10% gels (Epizyme, Shanghai, China) and transferred to polyvinylidene difluoride membranes. We cut the membranes horizontally into strips for detecting proteins with different molecular weights. The membranes were blocked with blocking buffer (Biosharp) for 1–4 h and incubated with primary antibody for 12 h at 4°C. Next, the membranes

Table 1 The Primer Sequences

Gene	Primer Sequences (5'-3')
SOX9	AGTACCCGCATCTGCACAAC
	ACGAAGGGTCTCTTCTCGCT
Aggrecan	AGGTGTCGCTCCCCAACTAT
	CTTCACAGCGGTAGATCCCAG
MMP3	TTAAAGACAGGCACTTTTGGCG
	CCCTCGTATAGCCCAGAACT
ADAMTS5	CGCTACACTCTAAAGCCACTC
	CCTCGAAGCTAAAGCCCTCG
NFATc1	CCGTTGCTTCCAGAAAATAACA
	TGTGGGATGTGAACTCGGAA
c-Fos	CCAGTCAAGAGCATCAGCAA
	CCAGTCAAGAGCATCAGCAA
ACP5	CACTCCCACCCTGAGATTTGT
	CCCCAGAGACATGATGAAGTCA
CTSK	CTTCCAATACGTGCAGCAGA
	TCTTCAGGGCTTTCTCGTTC
V-ATPaseD2	AAGCCTTTGTTTGACGCTGT
	TTCGATGCCTCTGTGAGATG
DC-STAMP	AAAACCCTTGGGCTGTTCTT
	AATCATGGACGACTCCTTGG
GAPDH	ACCCAGAAGACTGTGGATGG
	ACCCAGAAGACTGTGGATGG

were incubated with secondary antibody for 1 h at room temperature, followed by the detection of target proteins with an ultra-sensitive ECL chemiluminescence kit (NCM Biotech, Suzhou, China) and the ImageQuant LAS 500 system (GE Healthcare, Fairfield, CT, USA). The intensity of each band was quantified by ImageJ software (Bethesda, MD, USA) and normalized using β-actin.

Immunofluorescence

After cells reaching 50% density, ATDC5 and BMMs were fixed in 4% paraformaldehyde for 15 min. The fixed cells were permeabilized with 0.2% Triton X-100 for 20 min and blocked at room temperature for 30 min, followed by the incubation of cells in primary antibody at 4°C overnight and secondary antibody at room temperature for 1 h. The nuclei were stained with DAPI, and the cells were viewed by confocal microscopy.

Animal Model

8-week-old male C57BL/6J mice were randomly divided as follows: sham-operated group, OA group, OA + 5 mg/kg paroxetine group, and OA + 20 mg/kg paroxetine group (n = 6/group). Mouse osteoarthritis model constructed with destabilization of the medial meniscus (DMM) surgery. After all mice were anesthetized with inhalation of 3% isoflurane, the medial meniscus-tibial ligament (MML) was exposed by making an incision next to the medial knee ligament. For OA and OA + paroxetine treatment groups, the MML was excised to destabilize of the medial meniscus. The MML was intact in the sham-operated group. After surgery, the mice were treated intraperitoneally with different drugs for 8 weeks, while the sham-operated and OA groups were treated with phosphate buffered saline on alternate days.

Histological Observations and Immunohistochemistry

The knee joints (n = 6/group) were fixed in 4% paraformaldehyde for 24 h and decalcified with 10% EDTA solution for 4 weeks. Paraffin-embedded tissues were cut into 5-μm-thick sections and stained with hematoxylin-eosin (HE), safranin

O-fast green (SO), or TRAP. The degree of cartilage degeneration was assessed according to the Osteoarthritis Research Society International (OARSI) scoring system.[34] The TRAP-positive cell number were recorded.

For immunohistochemistry experiments, sections (n = 6/group) were deparaffinized in xylene and rehydrated in gradient ethanol. We incubated the sections with 3% H_2O_2 and 5% bovine serum albumin at room temperature. The primary antibodies (Aggrecan, MMP3, Nlrp3) were incubated overnight at 4°C. Subsequently, sections were incubated with secondary antibodies conjugated to horseradish peroxidase and counterstained with hematoxylin. The positive cell staining rates were statistically analyzed with ImageJ.

Statistical Analysis

GraphPad Prism 5.0 software (GraphPad Software, La Jolla, CA, USA) was used for data processing. One-way analysis of variance (ANOVA) was used for comparisons of means among three or more groups, and Student's *t*-test was used for comparisons of means between two groups. All experiments were performed at least three independent times, and p-values < 0.05 were considered statistically significant.

Results

Effect of Paroxetine on ATDC5 Cytotoxicity

The chemical formula of paroxetine is shown in Figure 1A. The CCK8 assay results demonstrated that paroxetine had cytotoxic effects on ATDC5 cells at a concentration of 10 μM after 24 and 48 h of treatment (Figure 1B). The IC_{50} values of paroxetine for ATDC5 cells were determined to be 12.01 μM at 24 hours and 7.56 μM at 48 hours. Concentrations below 5 μM did not exhibit cytotoxicity and were considered safe for ATDC5 treatment. Therefore, in subsequent experiments, we used paroxetine concentrations of 1.25, 2.5, and 5 μM.

Effects of Paroxetine on the Homeostasis of the Extracellular Matrix (ECM) in IL-1β-Stimulated ATDC5 Cells

Next, we investigated the effects of paroxetine on the synthesis and catabolism of extracellular matrix components in ATDC5 cells. The toluidine blue staining results showed a decrease in the area of the extracellular matrix in ATDC5 cells after treatment with IL-1β (Figure 1C–D). However, paroxetine could rescue the effects of IL-1β on the extracellular matrix, showing the strongest protective effect at a concentration of 2.5 μM.

To further investigate the effect of Paroxetine on the expression of anabolic and catabolic-related proteins, we performed Western blot assays on ATDC5 cells. As shown in Figure 1E–H, the protein levels of aggrecan and SOX9 were reduced in response to IL-1β treatment. Paroxetine treatment inhibited IL-1β-induced anabolic suppression. In particular, the most prominent promotion of the ECM synthesis was observed at a concentration of 2.5 μM. In addition, paroxetine suppressed the expression of MMP3 and ADAMTS5, thereby exhibiting an inhibitory effect on catabolism (Figure 1F, I and J). Meanwhile, we detected the mRNA expression levels of the above genes by RT-PCR (Figure 1K). The results were consistent with Western blot, indicating that paroxetine treatment was able to upregulate the anabolic-related protein expression and suppress the catabolic-related protein expression. Taken collectively, the data indicate that paroxetine has a protective effect on the homeostasis of the extracellular matrix in ATDC5 cells.

Paroxetine Alleviates IL-1β-Induced Pyroptosis by Inhibiting NF-κB Signaling Pathway Activation in ATDC5 Cells

Pyroptosis is associated with inflammation and cartilage degeneration.[35,36] Chondrocytes were treated with IL-1β and different concentrations of paroxetine, and the protein levels of pyroptosis-related proteins were examined by Western blotting. As shown in Figure 2A–H, the protein levels of Nlrp3, clv-IL-1β, and clv-caspase1 were significantly increased after IL-1β treatment, indicating that the pyroptosis-related pathway is activated. However, treatment with paroxetine reversed this phenomenon in a dose-dependent manner. The protein level expression of Nlrp3, clv-caspase1 and clv-IL-1β was significantly downregulated in the paroxetine treated group. Moreover, we observed the formation of Nlrp3 inflammasome in ATDC5 cells under confocal microscopy (Figure 2I). The results showed that inflammasome formation

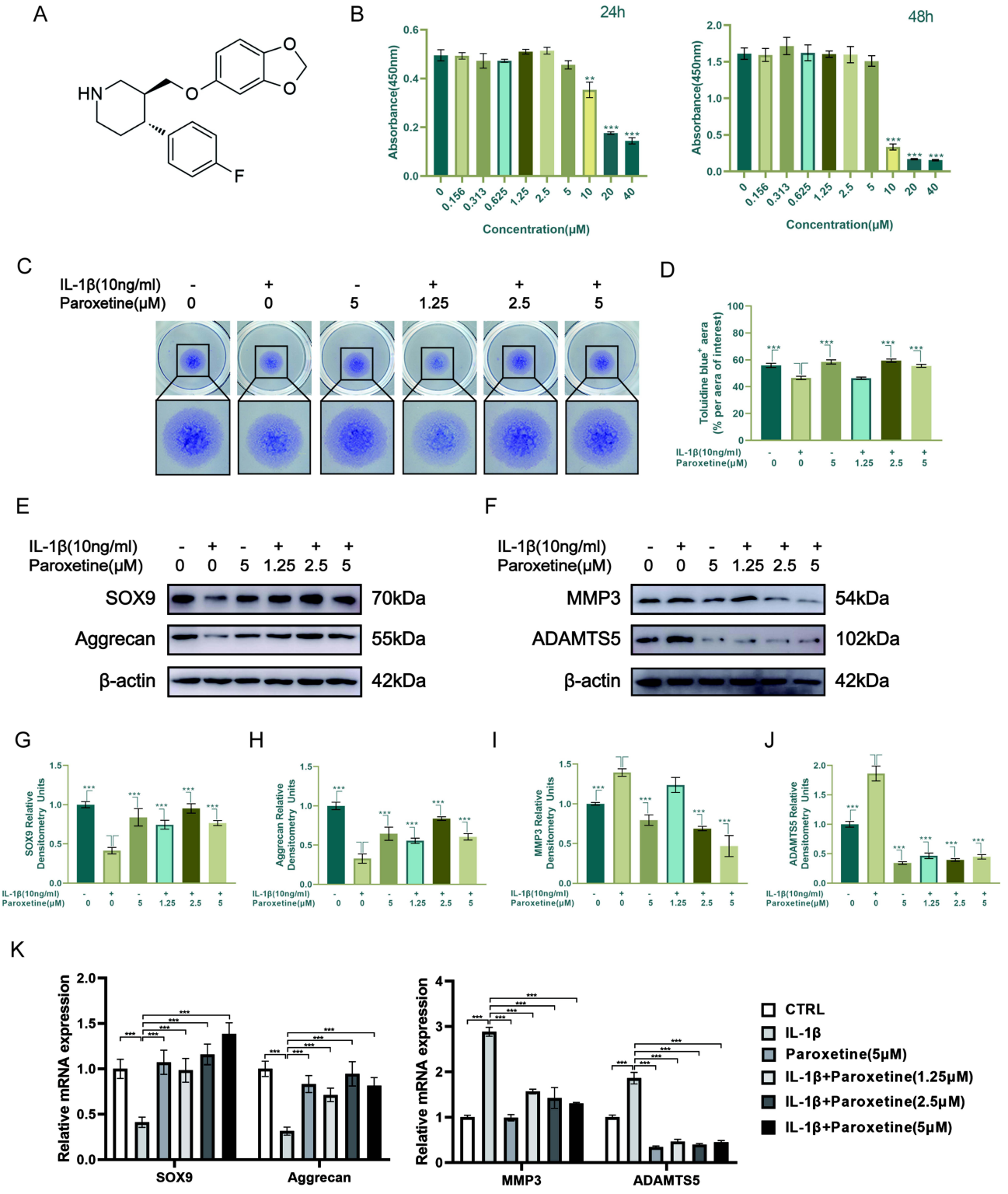

Figure 1 Paroxetine promotes extracellular matrix synthesis and inhibits catabolism. (**A**) Chemical structure of paroxetine. (**B**) Cytotoxic effects of paroxetine in ATDC5 cells after treatment for 24 and 48 h. (**C**) Toluidine blue staining of high-density-cultured ATDC5 cells after treatment with different concentrations of paroxetine and IL-1β. (**D**) Toluidine blue (+) area (%/area of interest) analysis as quantified by ImageJ. (**E–J**) Western blotting results of extracellular matrix anabolic- and catabolic-related proteins (SOX9, Aggrecan, MMP3, ADAMTS5) in ATDC5 cells as quantified by ImageJ. (**K**) The expression levels of genes related to extracellular matrix synthesis and catabolism were quantified by RT-PCR. Data are presented as mean ± S.D. (n = 3/group). Significant differences between groups are indicated as ***$p < 0.001$, **$p < 0.01$.

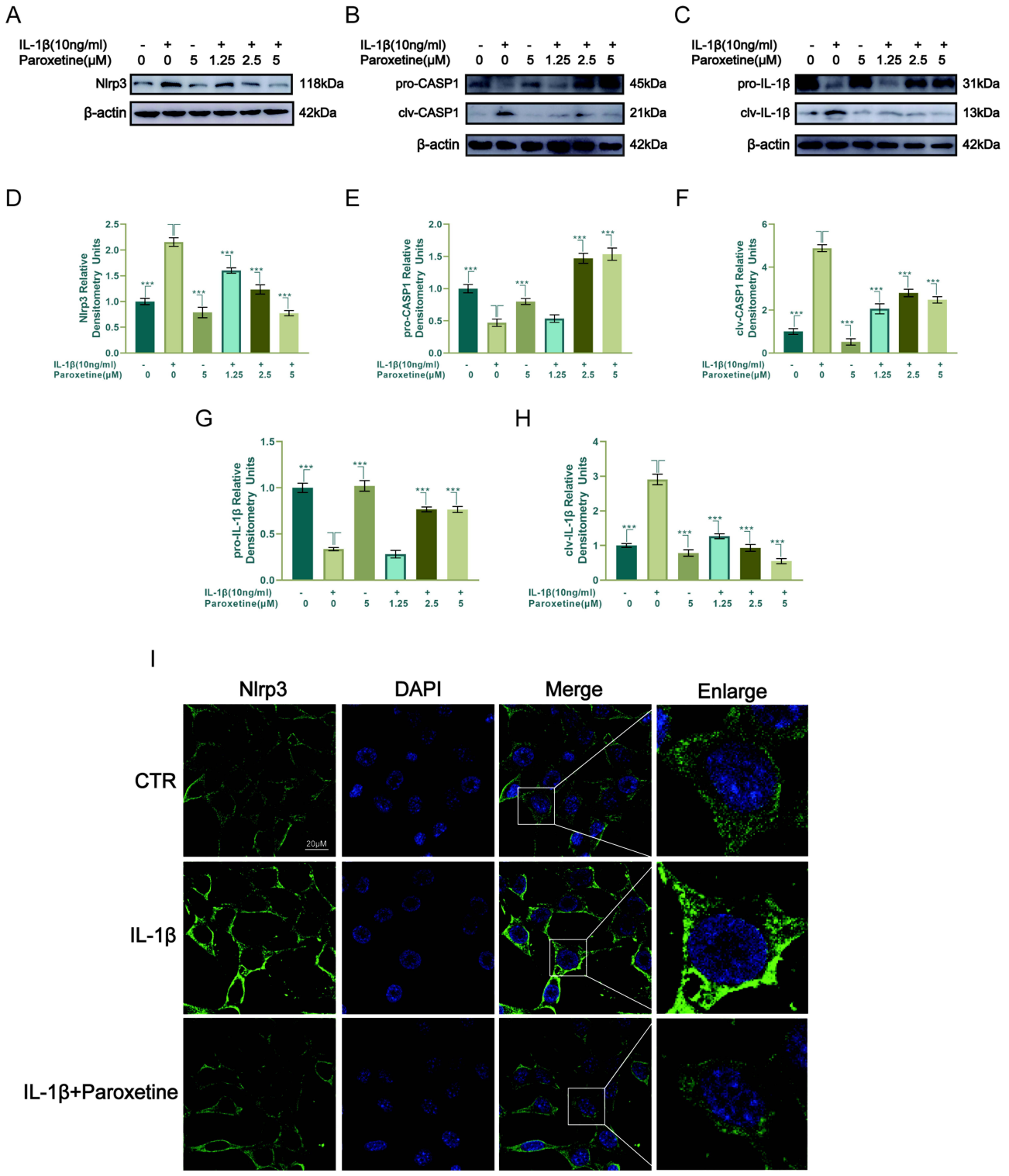

Figure 2 Paroxetine alleviates IL-1β-induced pyroptosis in ATDC5. (**A**–**C**) Western blotting results of pyroptosis-related proteins (Nlrp3, IL-1β and Caspase1 [CASP1]). (**D**–**H**) Protein levels were quantified by ImageJ. (**I**) Nlrp3 was assessed by immunofluorescence staining combined with DAPI staining. Values are mean ± SD (n = 3/group). Significant differences between groups are indicated as ***$p < 0.001$.

was more abundant and brighter under IL-1β treatment. However, in the paroxetine treated group, inflammasome forming was significantly repressed, which is consistent with previous Western blot results showing the inhibition of pyroptosis - related pathways.

To further investigate the potential mechanism of pyroptosis inhibition by paroxetine, we observed the effect of paroxetine on NF-κB signaling pathway. The NF-κB signaling pathway mediates the IL-1β-stimulated inflammatory response. As shown in Figure 3A–E, the results indicated that the NF-κB signaling pathway was activated under IL-1β treatment, as evidenced by elevated expression of p-IκB and p-P65 and significantly reduced expression of IκB. In paroxetine-treated ATDC5, the levels of p-P65 and p-IκB were suppressed, and IκB degradation was decreased. Moreover, after IL-1β treatment, P65 immunofluorescence results showed increased translocation of P65 into the nucleus

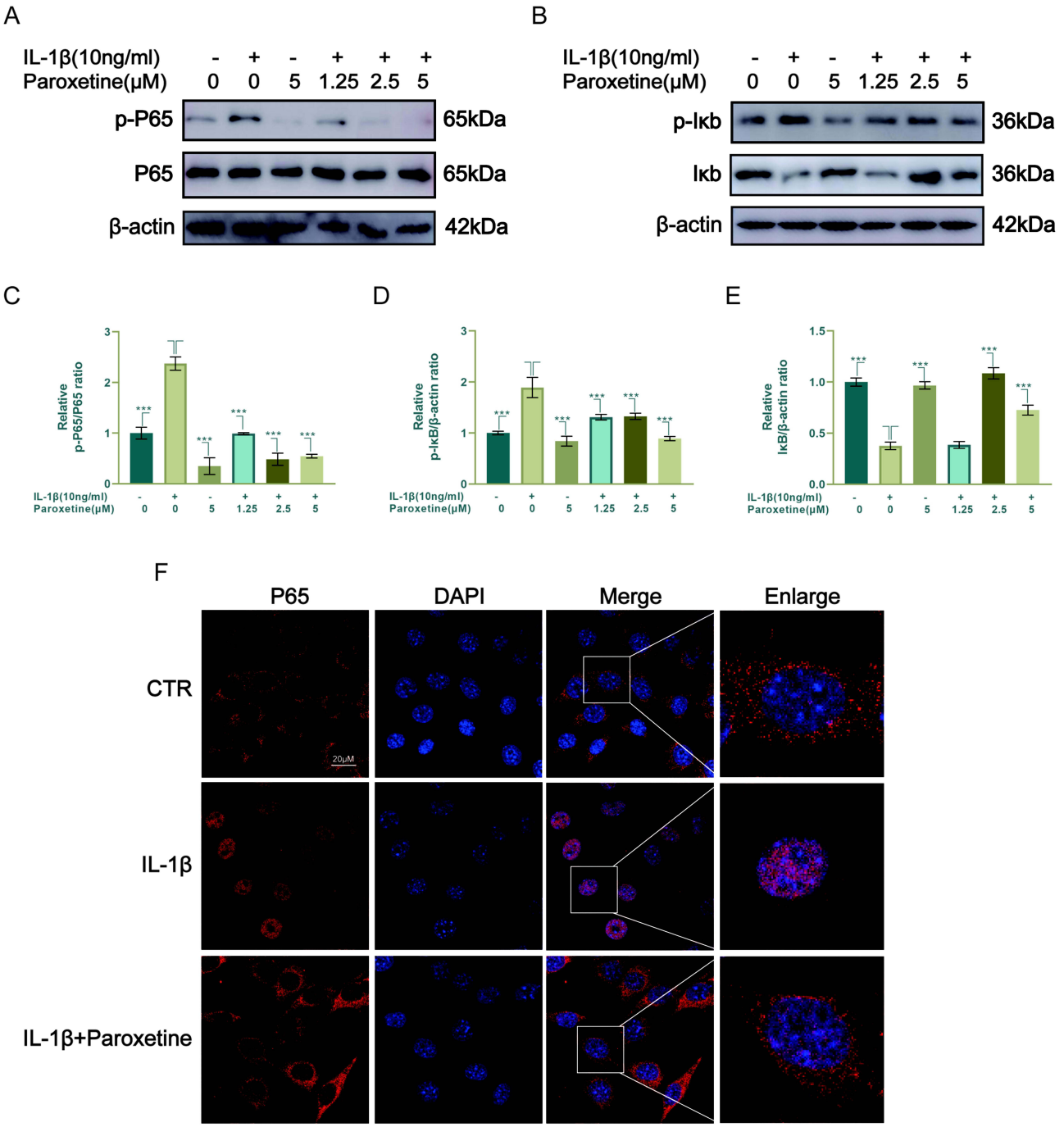

Figure 3 Paroxetine inhibits NF-κB signaling pathway activation in ATDC5. (**A**–**E**) Western blotting results of NF-κB-related signaling pathway proteins (p-P65, P65, p-IκB and IκB). (**F**) P65 localization was assessed by immunofluorescence. Values are mean ± SD (n = 3/group). Significant differences between groups are indicated as ***$p < 0.001$.

(Figure 3F). However, P65 was highly localized in the cytoplasm in paroxetine-treated cells. These results suggest that paroxetine can alleviate IL-1β-induced pyroptosis by inhibiting NF-κB signaling pathway activation in ATDC5 cells.

Paroxetine Inhibits Osteoclast Formation in vitro

After treating BMMs with different concentrations of paroxetine for 48 and 96 h, the cell viability was evaluated (Figure 4A). Paroxetine exhibited IC_{50} values of 9.29 μM at 48h and 4.86 μM at 96h on BMMs. After 96 hours of treatment with 2.5 μM paroxetine, there were no signs of cytotoxicity in BMMs. Therefore, in our subsequent experiments, we used concentrations of 0.625, 1.25, and 2.5 μM. To observe the effects of paroxetine on osteoclast formation, BMMs were treated with RANKL and different concentrations of paroxetine for 6 days and processed for TRAP staining. As shown in Figure 4B–D, BMMs differentiated into mature osteoclasts in the presence of RANKL. However, paroxetine inhibited this phenomenon, and the number and area of osteoclasts decreased as the drug concentration increased. At a concentration of 2.5 μM, paroxetine displayed the strongest effect in preventing osteoclast formation. To observe the protective effects of paroxetine at different phases of osteoclast differentiation, BMMs were treated with paroxetine at a concentration of 2.5 μM at early (1–3 days), middle (3–5 days), and late (5–7 days) stages of differentiation. The strongest inhibitory effect was observed at the early stage of differentiation, and the treatment of cells with paroxetine at the late stage of differentiation had no significant protective effect in the osteoclast profile compared to RANKL treatment (Figure 4E–G). Consistent with the results of TRAP staining, the number and size of F-actin rings also decreased in response to paroxetine treatment (Figure 4H–J).

Next, the effects of paroxetine on the RANKL-induced expression of bone-remodeling-related genes were examined. After 6 days of treatment with RANKL and different concentrations of paroxetine, the RT-PCR results showed that the levels of osteoclast-associated genes (c-Fos, NFATc1, ACP5, V-ATPase D2, DC-STAMP, and CTSK) were decreased in a concentration-dependent manner (Figure 5A). NFATc1, one of the downstream transcription factors of the NF-κB signaling pathway, plays important roles in osteoclast formation and function. Paroxetine had a pronounced inhibitory effect on NFATc1 protein expression (Figure 5B and C).

In conclusion, the above results on in vitro experiments showed a significant inhibitory effect of paroxetine on osteoclast formation.

Paroxetine Inhibits the Activation of the RANKL-Stimulated NF-κB Signaling Pathway

To understand the mechanism by which paroxetine inhibits osteoclast formation, the levels of proteins associated with the NF-κB signaling pathway were examined by Western blotting. As shown in the Figure 5D–H, in response to RANKL stimulation, the levels of p-P65 and p-IκB were significantly elevated, indicating activation of the NF-κB pathway. Notably, paroxetine could inhibit the increase in the levels of p-P65 and p-IκB and prevent the degradation of IκB in a concentration-dependent manner. P65 immunofluorescence showed that paroxetine treatment suppressed RANKL-induced P65 translocation to the nucleus, which would lead to the inhibition of NF-κB activation (Figure 5I).

Taken collectively, these findings indicate that paroxetine inhibits NF-κB by reducing IκB degradation and inhibiting p65 nuclear translocation, which prevents osteoclast formation.

Paroxetine Protects Chondrocytes and Inhibits Osteoclast Formation in vivo

To examine the protective effect of paroxetine in the development of OA, we performed transection of the medial meniscal tibial ligament in mice to simulate an osteoarthritis model, supplemented with 5 mg/kg and 20 mg/kg paroxetine injections intraperitoneally. HE and SO staining was performed to observe the structure of the knee joint and assess the extent of cartilage degeneration (Figure 6A). The thickness of the cartilage and its surface smoothness are crucial factors in determining the severity of cartilage degeneration. The results of histological staining demonstrated that the mice subjected to DMM surgery exhibited a decrease in proteoglycan content and a thinner layer of cartilage. In comparison to the sham-operated group, the DMM group displayed a rougher surface on the knee joint cartilage. However, the mice in the paroxetine-treated group exhibited an increased thickness of the cartilage layer staining and a flatter joint surface in their knee joints. This suggests that the degeneration of cartilage was reduced in the DMM mice treated with paroxetine, and this effect was particularly noticeable in the group treated with a higher concentration. In

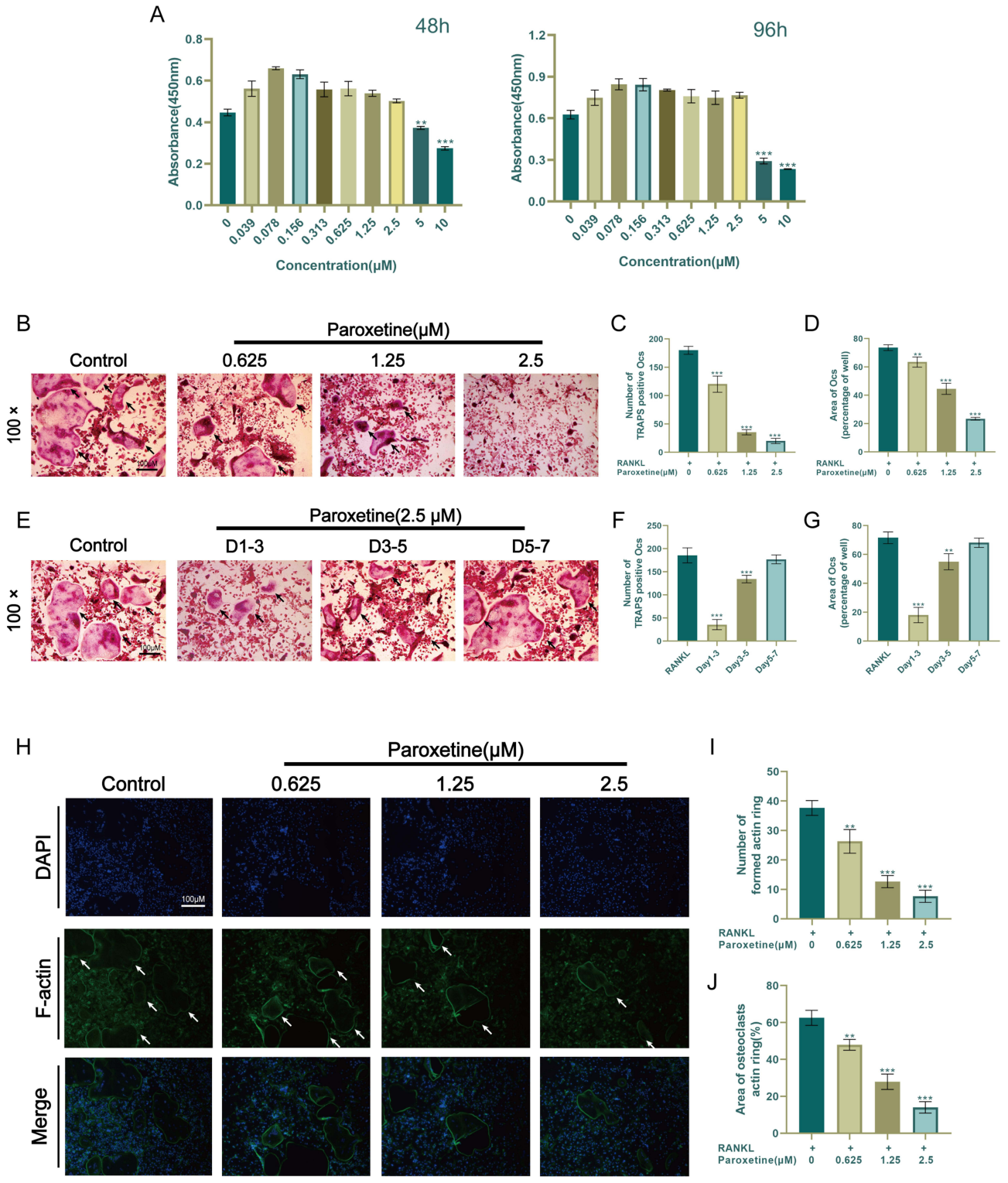

Figure 4 Paroxetine inhibits RANKL-induced osteoclast differentiation in vitro. (**A**) Cytotoxic effects of paroxetine in BMMs after treatment for 48 and 96 h. (**B**–**D**) TRAP staining of BMMs to observe the effects of different concentrations of paroxetine on RANKL-induced osteoclastic differentiation. (**E**–**G**) BMMs were treated with paroxetine for different periods of time to counteract the effects of RANKL. (**H**–**J**) F-actin rings were observed in osteoclasts by confocal microscopy. Osteoclasts with F-actin rings are marked with white arrows. Values are mean ± SD (n = 3/group). Significant differences between groups are indicated as ***$p < 0.001$, ** $p < 0.01$, and * $p < 0.05$.

addition, we observed the uniformity of cartilage tissue staining in the arthritis model, which is also one of the important indicators for evaluating the degree of cartilage degradation in the OA model.[37] The results of SO staining (bright red areas represent stained cartilage) showed that compared to the DMM group, the paroxetine-treated group exhibited

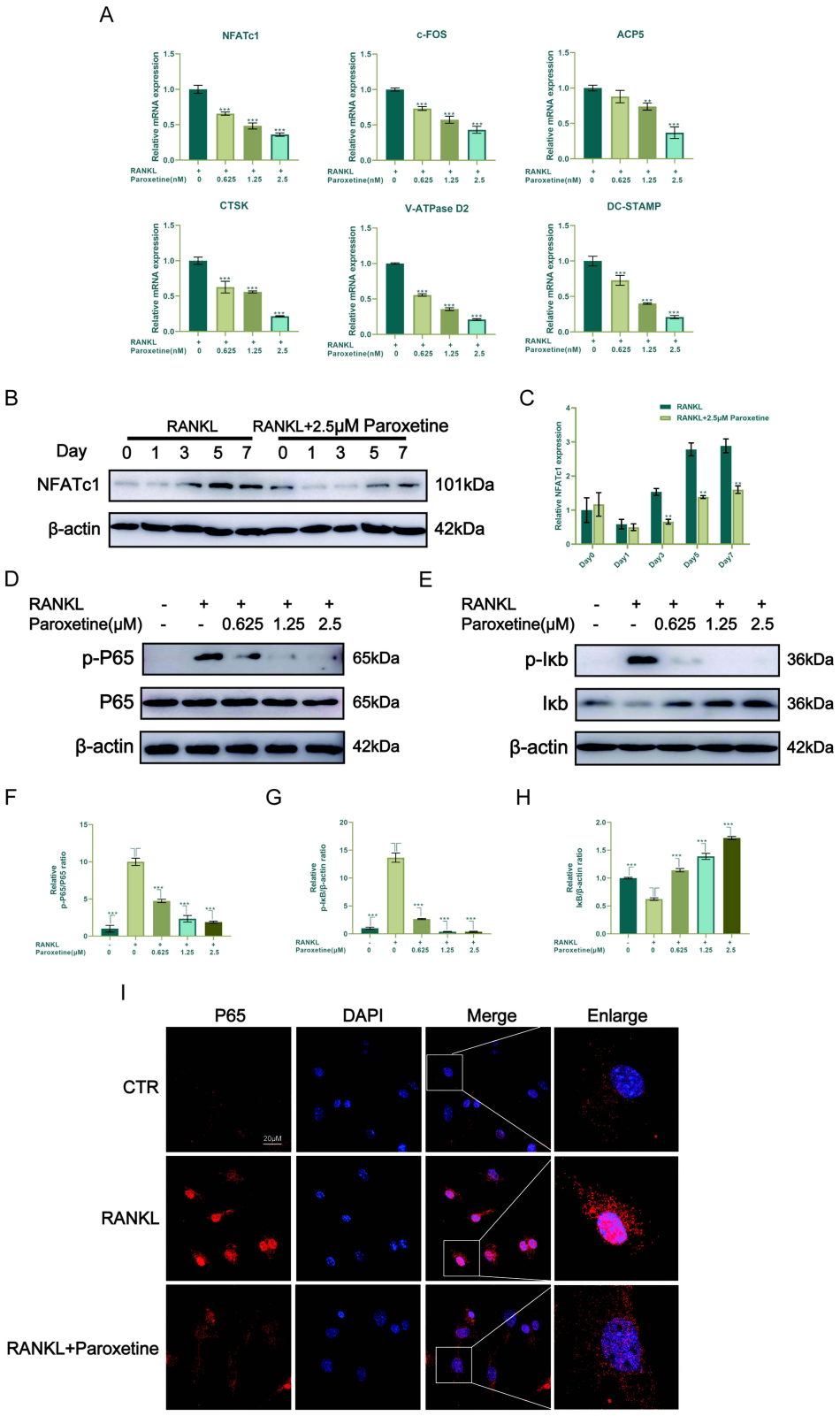

Figure 5 Paroxetine inhibits osteoclast formation by suppressing the NF-κB signaling pathway. (**A**) RT-PCR results of osteoclast-related genes. (**B**–**H**) Western blotting results of NFATc1 and NF-κB signaling pathway-related proteins (p-P65, P65, p-IκB and IκB). (**I**) P65 localization was assessed by immunofluorescence. Values are mean ± SD (n = 3/group). Significant differences between groups are indicated as ***$p < 0.001$ and ** $p < 0.01$.

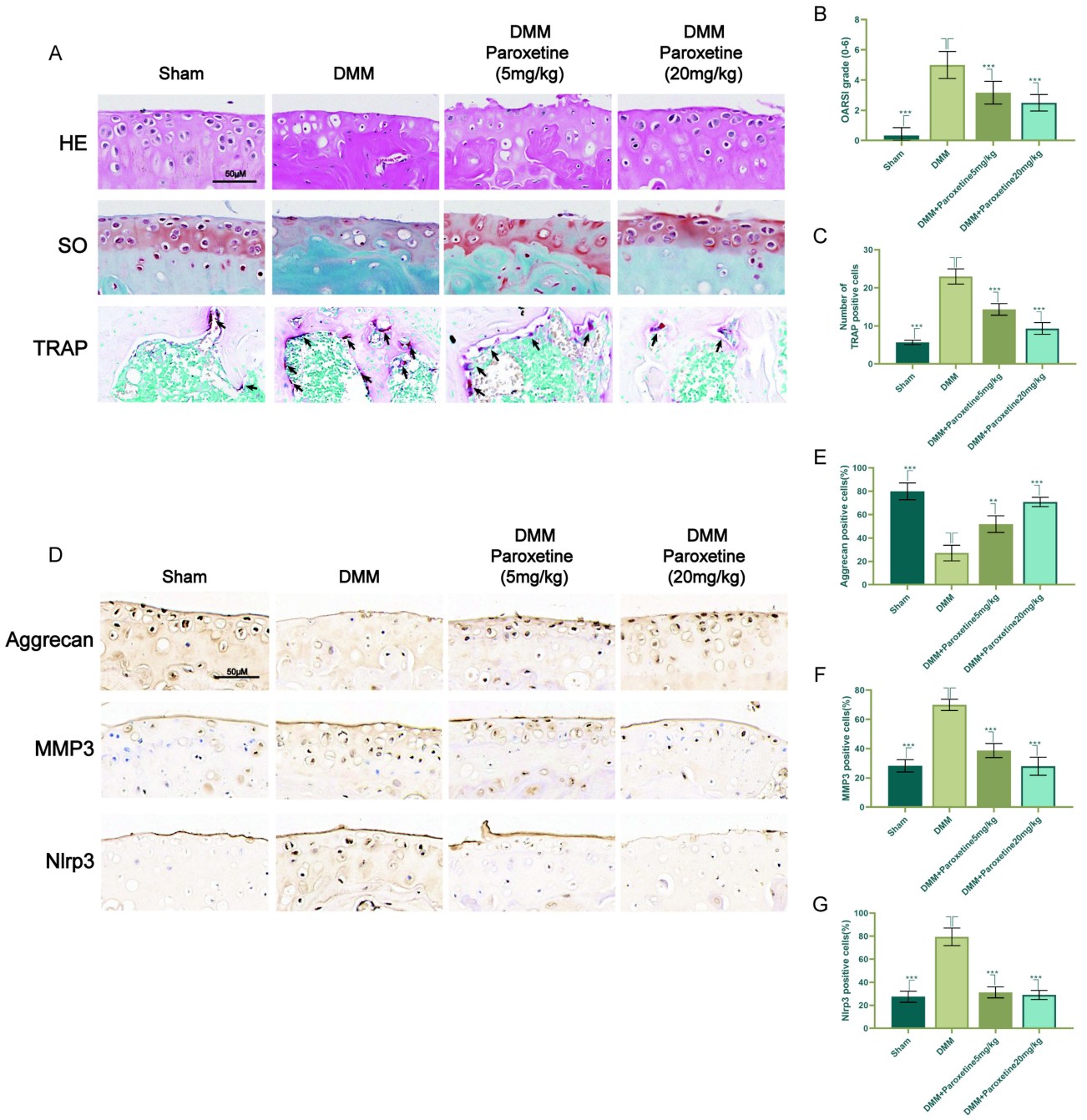

Figure 6 Paroxetine delays the progression of osteoarthritis in murine DMM model. (**A**) Sections of knee joints were stained with HE, SO, and TRAP. (**B**) OARSI scores of cartilage specimens of different groups. (**C**) TRAP positive number were recorded. (**D**–**G**) Aggrecan, MMP3, and Nlrp3 expression levels in mouse cartilage were assessed by immunohistochemistry. The positive cell staining rates were statistically analyzed with ImageJ. Values are mean ± SD (n = 3/group). Significant differences between groups are indicated as ***$p < 0.001$ and ** $p < 0.01$.

a more uniform positive staining in the cartilage layer. The OARSI scores were used to confirm the condition of the joints in the OA model mice.[34] The results, as shown in Figure 6B, indicated that the DMM mice had lower OARSI scores after being treated with paroxetine. This suggests that paroxetine can effectively prevent the degradation of cartilage matrix and reduce cartilage degeneration. The results of TRAP staining showed increased osteoclast formation in the subchondral bone in mice with destabilized medial meniscus. The number of osteoclasts staining positive for TRAP decreased after paroxetine treatment (Figure 6A and C). In addition, paroxetine inhibited osteoclast formation, which is consistent with the in vitro results, thereby impeding bone loss.

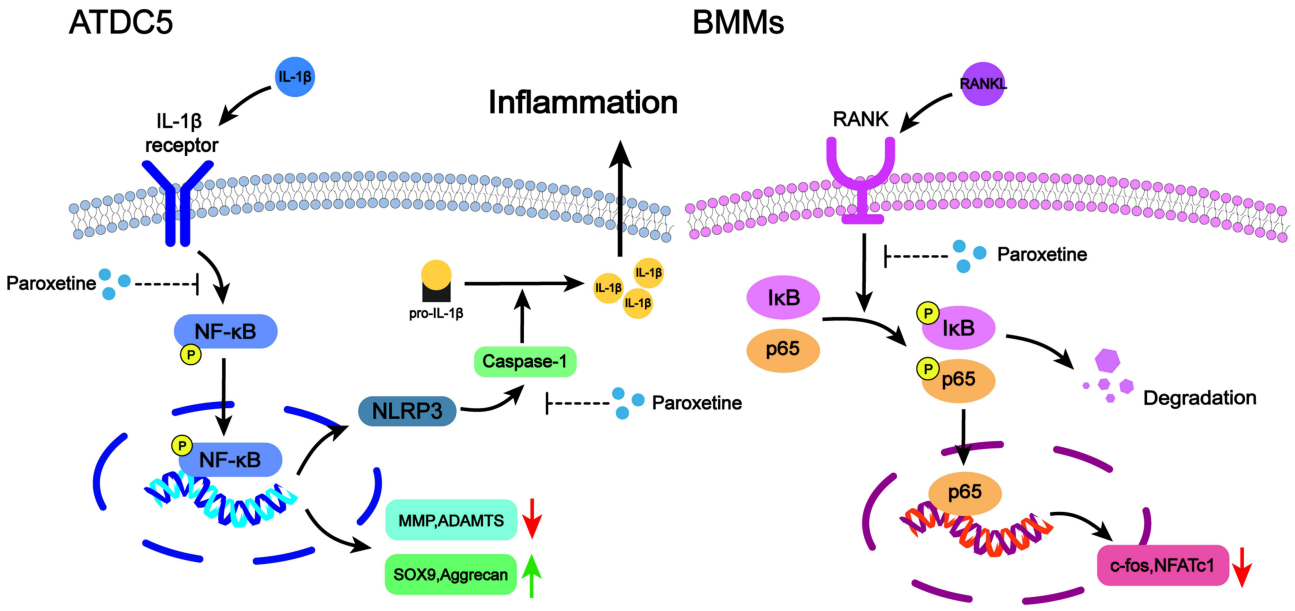

Figure 7 Mechanism by which paroxetine delayed the progression of osteoarthritis. Paroxetine was capable of attenuating chondrocyte pyroptosis and reducing osteoclast formation via inhibiting NF-κB pathway.

In addition, we performed immunohistochemical staining of cartilage tissues for Aggrecan, MMP3, and Nlrp3. The results showed that the number of Aggrecan-positive cells was significantly higher in the paroxetine injection group than in the DMM group, while the number of MMP3 and Nlrp3-positive cells was significantly lower (Figure 6D–G). This suggests that paroxetine promotes extracellular matrix synthesis and inhibits the activation of catabolic and pyroptosis-related pathways in vivo. The relevant molecular mechanisms are shown in Figure 7, our findings demonstrate that paroxetine protects chondrocytes and inhibits osteoclast formation by inhibiting the NF-κB signaling pathway, and it has the potential to be an effective agent in the treatment of osteoarthritis.

Discussion

Osteoarthritis is associated with age-related degeneration, the immune response, and trauma, and it is characterized by structural changes that attack the entire joint, including the hyaline articular cartilage, subchondral bone, joint capsule, synovial membrane, and periarticular muscles.[11,38,39] The high prevalence of OA has become a major public health problem, affecting an increasing number of individuals and leading to disability.[40] Unfortunately, the pathogenesis of OA is unknown, and the majority of patients with OA do not receive appropriate treatment, regardless of the stage of the disease. Previous studies have demonstrated that paroxetine, known for its strong and specific inhibition of GRK2, has the potential to delay osteoarthritis degeneration.[33] We believe that further exploration of the potential mechanisms underlying the protective effect of paroxetine is of great significance for its use in the clinical treatment of osteoarthritis.

The degradation of the extracellular matrix of articular chondrocytes plays a crucial role in the development of OA.[2,41] Under normal conditions, anabolic and catabolic processes maintain the homeostasis of the extracellular matrix. IL-1β, as a classical stimulator, has been shown to induce inflammatory responses in chondrocytes and promote senescence and apoptotic changes in primary chondrocytes.[37,42,43] In the present experiment, we used IL-1β to establish an in vitro model of OA to observe the protective effect of paroxetine on chondrocytes. We observed that IL-1β treatment increased the expression of catabolic-related proteins (MMP3, ADAMTS5) in ATDC5 cells, while the levels of SOX9 and aggrecan decreased. However, in the paroxetine treatment group, the damaging effect of IL-1β on chondrocytes was suppressed, exhibiting more extracellular matrix synthesis. Moreover, consistent with the Western blot and RT-PCR results, after paroxetine treatment, high-density cultured ATDC5 cells were capable of attenuating IL-1β-induced extracellular matrix metabolic disorders and exhibited more matrix synthesis.

Previous research has shown that abnormal activation of NF-κB transcription factors occurs during the development of osteoarthritis, triggered by various factors such as pro-inflammatory cytokines, inflammatory mediators, and extracellular matrix degradation products.[44] The activation of NF-κB signaling pathway inhibits chondrocyte anabolism, promotes the expression of multiple matrix degradation proteases, and leads to chondrocyte apoptosis.[18] In the present study, we demonstrated that paroxetine treatment was able to inhibit IL-1β-induced NF-κB signaling pathway activation, as evidenced by reduced expression levels of p-IκB and p-P65 and decreased IκB degradation. Moreover, immunofluorescence results showed that paroxetine was able to inhibit P65 nuclear translocation in ATDC5 cells.

The inhibitory effect of paroxetine on the NF-κB pathway may be an important mechanism for its ability to attenuate NLRP3 inflammasome-mediated chondrocyte pyroptosis in the progression of osteoarthritis. The NF-κB signaling pathway is a significant mediator of the pro-inflammatory response and plays a central role in the aggregation of NLRP3 components and the formation of NLRP3 inflammasome activation.[45–47] In the present study, we examined the expression levels of pyroptosis-related proteins by Western blot. The results showed that paroxetine treatment decreased the expression levels of Nlrp3, clv-IL-1β, and clv-caspase1 and reduced Nlrp3 inflammasome formation in immunofluorescence. In conclusion, paroxetine treatment was able to attenuate chondrocyte pyroptosis in the progression of osteoarthritis by inhibiting NF-κB signaling pathway activation.

Recently, growing evidence supported the role of subchondral bone homeostasis in the onset and progression of OA.[48,49] Under normal physiological conditions, subchondral bone dynamically adjusts the mechanical forces exerted on the joint via tightly coupled activity of osteoclasts and osteoblasts.[12] Nevertheless, during the progression of osteoarthritis, there is a continued increase in subchondral bone remodeling.[11] This includes an increase in sensory nerves within the subchondral bone and a heightened sensitivity to pain, which is believed to be associated with osteoclast activity.[14] Given the crucial role of subchondral osteoclasts in the progression of osteoarthritis, they present a promising target for pharmacological intervention. In this study, we investigated the mechanism of action of paroxetine in osteoclast formation. The expression of NF-κB signaling pathway proteins was examined by Western blotting, and the results showed that paroxetine could inhibit the increase in the levels of p-P65 and p-IκB in the presence of RANKL and prevent the degradation of IκB. The activation of the NF-κB signaling pathway was inhibited in a concentration-dependent manner. In addition, NFATc1, a downstream transcription factor of the NF-κB signaling pathway, plays important roles in osteoclast formation and function. Paroxetine had a significant inhibitory effect on NFATc1 expression at both protein and mRNA levels. Furthermore, the expression levels of other genes related to osteoclasts, including c-Fos, ACP5, V-ATPase D2, DC-STAMP, and CTSK, were also decreased upon treatment with paroxetine. To assess the impact of paroxetine on osteoclast formation, we employed TRAP and F-actin ring staining. The results indicated that the number and size of osteoclasts decreased with increasing concentrations of paroxetine treatment. Taken together, these findings imply paroxetine is capable of reducing osteoclast formation by inhibiting NF-κB signaling pathway activation.

To verify the protective effect of paroxetine on osteoarthritis in mice in vivo, we constructed an OA model with destabilization of the medial meniscus surgery. The results of histological staining demonstrated that mice subjected to DMM surgery exhibited a thinning of the cartilage layer and a rougher surface. However, after paroxetine treatment, especially in the high concentration treatment group, the cartilage layer of the knee joint surface stained thicker and more uniformly, and the surface was flatter. Moreover, similar to the in vitro experiments, the treatment with paroxetine suppressed the formation of subchondral osteoclasts induced by DMM surgery. The immunohistochemical analysis revealed that the paroxetine treated group exhibited increased levels of aggrecan expression, while MMP3 and Nlrp3 expression were decreased. In conclusion, paroxetine has the capability to maintain the balance of extracellular matrix metabolism in cartilage, attenuate pyroptosis, and inhibit osteoclast formation. These findings suggest that paroxetine has the potential to be an effective drug for osteoarthritis treatments.

However, there are some limitations to our study as well. First, the mouse DMM model used cannot fully reproduce the development of osteoarthritis in humans. Moreover, our choice of intraperitoneal administration is relatively less specific for treatment than local administration such as joint cavity injection. For this reason, we are considering combining paroxetine with a hydrogel that has better sustained release and biocompatibility for targeting localized treatment of the knee joint. These efforts will hopefully be refined in the future and allow for further exploration of paroxetine for clinical use in the treatment of osteoarthritis.

Conclusion

In conclusion, our findings show that paroxetine acts both in vivo and in vitro to protect chondrocytes and inhibit osteoclast formation. Moreover, the potential signaling pathways through which paroxetine acts are further revealed. The NF-κB and pyroptosis-related signaling pathways plays an important role in this protective effect. These findings suggest that paroxetine has potential as a new medication for osteoarthritis treatment. Future clinical studies are required to confirm the effect of paroxetine in OA progression.

Abbreviations

ADAMTS, A disintegrin and metalloproteinase with thrombospondin motifs; ASC, Apoptosis-associated spot-like protein containing CARD; BMMs, bone marrow-derived macrophages; DMM, destabilization of the medial meniscus; GRK2, G protein-coupled receptor kinase 2; HE, Hematoxylin-eosin staining; IL-1β, interleukin 1 beta; MMPs, Matrix metalloproteinases; NF-κb, Nuclear factor kappa-B; NLRP3, NOD-like receptor thermal protein domain associated protein 3; OA, Osteoarthritis; RANKL, Receptor activator of nuclear factor kappa-B ligand; SO, Safranine O-Fast Green staining; TRAP, Tartrate-resistant acid phosphatase staining.

Data Sharing Statement

The data used to support the findings of this study are included within the article.

Ethics Statement

All animal experiments were approved by the Animal Welfare and Ethics Committee of Taizhou Hospital, Wenzhou Medical University (No. tzy-2022151). The 3Rs guidelines for animal welfare were followed for in vivo studies.

Author Contributions

All authors made a significant contribution to the work reported, whether that is in the conception, study design, execution, acquisition of data, analysis and interpretation, or in all these areas; took part in drafting, revising or critically reviewing the article; gave final approval of the version to be published; have agreed on the journal to which the article has been submitted; and agree to be accountable for all aspects of the work.

Funding

This work was funded by the National Natural Science Foundation of China [No. 81272059], Natural Science Foundation of Zhejiang Province [No. LGF18H060012], Medical and Health Technology Program of Zhejiang Province [No. 2012KYA188], Medical Health Science and Technology Project of Zhejiang Provincial Health Commission [No. B2016KYB326], and Taizhou Social Development Science and Technology Project of Zhejiang Province [No. 21ywa54].

Disclosure

The authors declare no competing interests in this work.

References

1. Xie C, Sun Q, Dong Y, et al. Calcitriol-loaded multifunctional nanospheres with superlubricity for advanced osteoarthritis treatment. *ACS nano*. 2023;17(13):12842–12861. doi:10.1021/acsnano.3c04241
2. Rahmati M, Nalesso G, Mobasheri A, et al. Aging and osteoarthritis: central role of the extracellular matrix. *Ageing Res Rev*. 2017;40:20–30. doi:10.1016/j.arr.2017.07.004
3. Muthu S, Korpershoek JV, Novais EJ, et al. Failure of cartilage regeneration: emerging hypotheses and related therapeutic strategies. *Nat Rev Rheumatol*. 2023;19(7):403–416. doi:10.1038/s41584-023-00979-5
4. Wang W, Duan J, Ma W, et al. Trimanganese tetroxide nanozyme protects cartilage against degeneration by reducing oxidative stress in osteoarthritis. *Adv Sci*. 2023;10(17):e2205859. doi:10.1002/advs.202205859
5. Kolasinski S, Neogi T, Hochberg MC, et al. 2019 American College of Rheumatology/Arthritis Foundation guideline for the management of osteoarthritis of the hand, hip, and knee. *Arthritis Rheumatol*. 2020;72(2):220–233. doi:10.1002/art.41142

6. Lützner J, Kasten P, Günther K-P, et al. Surgical options for patients with osteoarthritis of the knee. *Nat Rev Rheumatol*. 2009;5(6):309–316. doi:10.1038/nrrheum.2009.88
7. Bannuru R, Osani MC, Vaysbrot EE, et al. OARSI guidelines for the non-surgical management of knee, Hip, and polyarticular osteoarthritis. *Osteoarthritis Cartilage*. 2019;27(11):1578–1589. doi:10.1016/j.joca.2019.06.011
8. Sun Z, Liu Q, Lv Z, et al. viaTargeting macrophagic SHP2 for ameliorating osteoarthritis TLR signaling. *Acta Pharm Sin B*. 2022;12(7):3073–3084. doi:10.1016/j.apsb.2022.02.010
9. Latourte A, Cherifi C, Maillet J, et al. Systemic inhibition of IL-6/Stat3 signalling protects against experimental osteoarthritis. *Ann Rheum Dis*. 2017;76(4):748–755. doi:10.1136/annrheumdis-2016-209757
10. Zheng X, Qiu J, Zhang H, et al. PD184352 exerts anti-inflammatory and antioxidant effects by promoting activation of the Nrf2/HO-1 axis. *Biochem Pharmacol*. 2023;211:115542. doi:10.1016/j.bcp.2023.115542
11. Hu W, Chen Y, Dou C, et al. Microenvironment in subchondral bone: predominant regulator for the treatment of osteoarthritis. *Ann Rheum Dis*. 2021;80(4):413–422. doi:10.1136/annrheumdis-2020-218089
12. Raggatt LJ, Partridge NC. Cellular and molecular mechanisms of bone remodeling. *J Biol Chem*. 2010;285(33):25103–25108. doi:10.1074/jbc.R109.041087
13. Zhang H, Wang L, Cui J, et al. Maintaining hypoxia environment of subchondral bone alleviates osteoarthritis progression. *Sci Adv*. 2023;9(14):eabo7868. doi:10.1126/sciadv.abo7868
14. Zhu S, Zhu J, Zhen G, et al. Subchondral bone osteoclasts induce sensory innervation and osteoarthritis pain. *J Clin Invest*. 2019;129(3):1076–1093. doi:10.1172/JCI121561
15. Guo Q, Chen X, Chen J, et al. STING promotes senescence, apoptosis, and extracellular matrix degradation in osteoarthritis via the NF-κB signaling pathway. *Cell Death Dis*. 2021;12(1):13. doi:10.1038/s41419-020-03341-9
16. Jimi E, Ghosh S. Role of nuclear factor-kappaB in the immune system and bone. *Immunol Rev*. 2005;208(1):80–87. doi:10.1111/j.0105-2896.2005.00329.x
17. Zheng X, Qiu J, Pan W, et al. Selumetinib - a potential small molecule inhibitor for osteoarthritis treatment. *Front Pharmacol*. 2022;13:938133. doi:10.3389/fphar.2022.938133
18. Choi MC, Jo J, Park J, et al. NF-κB signaling pathways in osteoarthritic cartilage destruction. *Cells*. 2019;8(7):734. doi:10.3390/cells8070734
19. Choi M, MaruYama T, Chun C-H, et al. Alleviation of murine osteoarthritis by cartilage-specific deletion of IκBζ. *Arthritis Rheumatol*. 2018;70(9):1440–1449. doi:10.1002/art.40514
20. Sueishi T, Akasaki Y, Goto N, et al. GRK 5 inhibition attenuates cartilage degradation via decreased NF -κB signaling. *Arthritis Rheumatol*. 2020;72(4):620–631. doi:10.1002/art.41152
21. Bergsbaken T, Fink SL, Cookson BT. Pyroptosis: host cell death and inflammation. *Nat Rev Microbiol*. 2009;7(2):99–109. doi:10.1038/nrmicro2070
22. Rao Z, Zhu Y, Yang P, et al. Pyroptosis in inflammatory diseases and cancer. *Theranostics*. 2022;12(9):4310–4329. doi:10.7150/thno.71086
23. Huang Y, Xu W, Zhou R. NLRP3 inflammasome activation and cell death. *Cell Mol Immunol*. 2021;18(9):2114–2127. doi:10.1038/s41423-021-00740-6
24. Elliott E, Sutterwala F. Initiation and perpetuation of NLRP3 inflammasome activation and assembly. *Immunol Rev*. 2015;265(1):35–52. doi:10.1111/imr.12286
25. Hochheiser IV, Behrmann H, Hagelueken G, et al. Directionality of PYD filament growth determined by the transition of NLRP3 nucleation seeds to ASC elongation. *Sci Adv*. 2022;8(19):eabn7583. doi:10.1126/sciadv.abn7583
26. Fu J, Wu H. Structural mechanisms of NLRP3 inflammasome assembly and activation. *Annu Rev Immunol*. 2023;41(1):301–316. doi:10.1146/annurev-immunol-081022-021207
27. He Y, Hara H, Núñez G. Mechanism and regulation of NLRP3 inflammasome activation. *Trends Biochem Sci*. 2016;41(12):1012–1021. doi:10.1016/j.tibs.2016.09.002
28. Kishi T, Ikuta T, Sakuma K, et al. Antidepressants for the treatment of adults with major depressive disorder in the maintenance phase: a systematic review and network meta-analysis. *Mol Psychiatry*. 2023;28(1):402–409. doi:10.1038/s41380-022-01824-z
29. Rickels K, Zaninelli R, McCafferty J, et al. Paroxetine treatment of generalized anxiety disorder: a double-blind, placebo-controlled study. *Am J Psychiatry*. 2003;160(4):749–756. doi:10.1176/appi.ajp.160.4.749
30. Nelson R, Guo Z, Halagappa V, et al. Prophylactic treatment with paroxetine ameliorates behavioral deficits and retards the development of amyloid and tau pathologies in 3xTgAD mice. *Exp Neurol*. 2007;205(1):166–176. doi:10.1016/j.expneurol.2007.01.037
31. Ning L, Wang X, Xuan B, et al. Identification and investigation of depression-related molecular subtypes in inflammatory bowel disease and the anti-inflammatory mechanisms of paroxetine. *Front Immunol*. 2023;14:1145070. doi:10.3389/fimmu.2023.1145070
32. Tai Y, Huang B, Guo -P-P, et al. TNF-α impairs EP4 signaling through the association of TRAF2-GRK2 in primary fibroblast-like synoviocytes. *Acta Pharmacol Sin*. 2022;43(2):401–416. doi:10.1038/s41401-021-00654-z
33. Carlson EL, Karuppagounder V, Pinamont WJ, et al. Paroxetine-mediated GRK2 inhibition is a disease-modifying treatment for osteoarthritis. *Sci Transl Med*. 2021;13(580):eaau8491. doi:10.1126/scitranslmed.aau8491
34. Pritzker KPH, Gay S, Jimenez SA, et al. Osteoarthritis cartilage histopathology: grading and staging - ScienceDirect. *Osteoarthritis Cartilage*. 2006;14(1):13–29. doi:10.1016/j.joca.2005.07.014
35. Chang X, Kang Y, Yang Y, et al. Pyroptosis: a novel intervention target in the progression of osteoarthritis. *J Inflamm Res*. 2022;15:3859–3871. doi:10.2147/JIR.S368501
36. An S, Hu H, Li Y, et al. Pyroptosis plays a role in osteoarthritis. *Aging Dis*. 2020;11(5):1146–1157. doi:10.14336/AD.2019.1127
37. Li G, Liu S, Chen Y, et al. An injectable liposome-anchored teriparatide incorporated gallic acid-grafted gelatin hydrogel for osteoarthritis treatment. *Nat Commun*. 2023;14(1):3159.
38. Zhang Y, Li S, Jin P, et al. Dual functions of microRNA-17 in maintaining cartilage homeostasis and protection against osteoarthritis. *Nat Commun*. 2022;13(1):2447. doi:10.1038/s41467-022-30119-8
39. Mapp P, Walsh D. Mechanisms and targets of angiogenesis and nerve growth in osteoarthritis. *Nat Rev Rheumatol*. 2012;8(7):390–398. doi:10.1038/nrrheum.2012.80

40. Loeser R, Collins J, Diekman B. Ageing and the pathogenesis of osteoarthritis. *Nat Rev Rheumatol*. 2016;12(7):412–420. doi:10.1038/nrrheum.2016.65
41. Peng Z, Sun H, Bunpetch V, et al. The regulation of cartilage extracellular matrix homeostasis in joint cartilage degeneration and regeneration. *Biomaterials*. 2021;268:120555. doi:10.1016/j.biomaterials.2020.120555
42. Arra M, Swarnkar G, Alippe Y, et al. IκB-ζ signaling promotes chondrocyte inflammatory phenotype, senescence, and erosive joint pathology. *Bone Res*. 2022;10(1):12. doi:10.1038/s41413-021-00183-9
43. Kang L, Yoon J, Rho JG, et al. Self-assembled hyaluronic acid nanoparticles for osteoarthritis treatment. *Biomaterials*. 2021;275:120967. doi:10.1016/j.biomaterials.2021.120967
44. Lepetsos P, Papavassiliou KA, Papavassiliou AG. Redox and NF-κB signaling in osteoarthritis. *Free Radic Biol Med*. 2019;132:90–100. doi:10.1016/j.freeradbiomed.2018.09.025
45. Zhang B, Chen H, Ouyang J, et al. SQSTM1-dependent autophagic degradation of PKM2 inhibits the production of mature IL1B/IL-1β and contributes to LIPUS-mediated anti-inflammatory effect. *Autophagy*. 2020;16(7):1262–1278. doi:10.1080/15548627.2019.1664705
46. Wang Q, Ou Y, Hu G, et al. Naringenin attenuates non-alcoholic fatty liver disease by down-regulating the NLRP3/NF-κB pathway in mice. *Br J Pharmacol*. 2020;177(8):1806–1821. doi:10.1111/bph.14938
47. Afonina I, Zhong Z, Karin M, et al. Limiting inflammation-The negative regulation of NF-κB and the NLRP3 inflammasome. *Nat Immunol*. 2017;18(8):861–869. doi:10.1038/ni.3772
48. Cui Z, Crane J, Xie H, et al. Halofuginone attenuates osteoarthritis by inhibition of TGF-β activity and H-type vessel formation in subchondral bone. *Ann Rheum Dis*. 2016;75(9):1714–1721. doi:10.1136/annrheumdis-2015-207923
49. Sun K, Guo Z, Hou L, et al. Iron homeostasis in arthropathies: from pathogenesis to therapeutic potential. *Ageing Res Rev*. 2021;72:101481. doi:10.1016/j.arr.2021.101481